2009

Carbon-nanotube biofiber microelectrodes

Carol M. Lynam
University of Wollongong, lynam@uow.edu.au

Gordon G. Wallace
University of Wollongong, gwallace@uow.edu.au

Willo Grosse
University of Wollongong, wmg896@uow.edu.au

Carbon-nanotube biofiber microelectrodes

Abstract

All-biocompatible carbon-nanotube fibers were formed using wet spinning. In this process the spinning solutions used are carbon nanotubes dispersed using biomolecules such as hyaluronic acid and chitosan. We compare the effect of a coagulation bath containing either a polymer binder, e.g., polyethyleneimine, or simply a precipitating solvent system, e.g., acetone. The electrical, mechanical, and morphological properties of the resulting fibers were studied. Biocompatible electrode structures were generated suitable for a variety of biomedical applications, e.g.,in biosensors or in systems where the application of an electrical field is advantageous e.g., stimulation of electrically excitable cells such as nerve and muscle cells.

Keywords

Carbon, nanotube, biofiber, microelectrodes

Publication Details

Lynam, C., Grosse, W. & Wallace, G. G. (2009). Carbon-nanotube biofiber microelectrodes. Electrochemical Society. Journal, 156 (7), 117-121.

Journal of The Electrochemical Society, **156** (7) P117-P121 (2009)
0013-4651/2009/156(7)/P117/5/$25.00 © The Electrochemical Society

Carbon-Nanotube Biofiber Microelectrodes

Carol Lynam,[z] Willo Grosse, and Gordon G. Wallace[*]

ARC Centre of Excellence for Electromaterials Science, Intelligent Polymer Research Institute, University of Wollongong, Wollongong NSW 2522, Australia

All-biocompatible carbon-nanotube fibers were formed using wet spinning. In this process the spinning solutions used are carbon nanotubes dispersed using biomolecules such as hyaluronic acid and chitosan. We compare the effect of a coagulation bath containing either a polymer binder, e.g., polyethyleneimine, or simply a precipitating solvent system, e.g., acetone. The electrical, mechanical, and morphological properties of the resulting fibers were studied. Biocompatible electrode structures were generated suitable for a variety of biomedical applications, e.g., in biosensors or in systems where the application of an electrical field is advantageous (e.g., stimulation of electrically excitable cells such as nerve and muscle cells).
 [DOI: 10.1149/1.3125799]

Manuscript submitted January 8, 2009; revised manuscript received March 30, 2009. Published May 14, 2009.

The unique electrical and mechanical properties of carbon nanotubes (CNTs) have attracted interest in their biological application both at the molecular and cellular levels.[1,2] The electrical properties of CNTs may permit them to be utilized to stimulate electrically excitable cells (nerve and muscle cells). Studies on interfacing CNTs with biomolecules have been of interest to function as platforms to support the growth of nerve cells.[3] It has been shown that varying the mechanical,[4] electrical,[5] and chemical[6] characteristics of surfaces influences neurite outgrowth rates and can even allow the control of neuron shape.

The possibility of employing CNTs as substrates able to improve neural signal transfer has been demonstrated by Lovat et al.[1] In another study, while neurons were found to extend neurites when grown on multiwalled carbon nanotubes (MWNTs),[3] more elaborate neurite branching was observed when neurons were grown on MWNTs functionalized with polyethyleneimine (PEI).[2] PEI is a widely used permissive substrate for nerve cells, supporting attachment and growth of neurons. Other molecules of interest are chitosan (CHIT) and hyaluronic acid (HA). CHIT and HA have independently shown to be effective in supporting the growth of a range of mammalian cell lines including osteoblasts[7,8] and nerve cells.[9,10] CHIT has also been blended with HA to form composite biomaterials for cartilaginous tissue scaffolds.[11] Recent innovative approaches to tissue repair involving these biomolecules have been developed.[12]

These studies imply that suitably functionalized CNTs could potentially be used in scaffolds to guide neurite outgrowth and highlight the opportunity available in combining CNTs with appropriate biomolecules. CNTs must be built into macroscopic structures to exploit their remarkable properties. Stable CNT dispersions exhibit liquid-crystalline behavior similar to conventional rodlike polymers in solution[13] (such as poly-paraphenylene terephthalamide) and so lend themselves to solution-spinning processing. The steps involved in wet spinning of CNTs present an ideal opportunity to introduce CNTs and biomolecules into practically useful structures. Vigolo et al.[14] dispersed CNTs in a surfactant-containing solution and then assembled the CNTs into long ribbons and fibers in a poly(vinyl alcohol) (PVA)-containing coagulation bath. Barisci et al.[15] developed this fiber-spinning process further by using DNA as the CNT dispersant and thereby adding biofunctionality to the fiber. However the fibers produced had electrical conductivity values several orders of magnitude lower than individual CNTs. Removing the polymer (PVA) binder in these fibers improved the electrical properties at great cost to the mechanical properties. Muñoz et al.[16] reported the use of surfactants as dispersants while employing a PEI coagulation bath to produce more highly conducting CNT fibers. Here we report the combination of using biocompatible molecules as dispersants and spinning into coagulation baths including PEI or acetone. This results in mechanically robust yet electrically conducting biomolecule-containing fibers.

Experimental

Materials.— All chemicals, single-wall CNTs (SWNTs, HiPCo produced from CNI), CHIT (Jakwang Co. Ltd.), HA (Sigma), PEI (Aldrich), acetone (Univar, Ajax Finechem), methanol (Univar, Ajax Finechem), potassium ferricyanide (Sigma), ferrocene monocarboxylic acid (Sigma), and ruthenium hexamine chloride (Sigma), were used as-received.

Instrumentation.— Scanning electron microscope (SEM) images were acquired using a Hitachi S-900 field-emission-scanning electron microscope (FESEM). Samples for FESEM were sputter coated with chromium before analysis. Raman spectroscopy measurements were performed using a Jobin Yvon Horiba HR800 spectrometer equipped with a He:Ne laser (λ = 632.8 nm) utilizing a 1800-line grating. Electrical conductivity measurements were carried out using the conventional four-point-probe method at room temperature. Electrochemical capacitance was calculated from the slope of anodic current amplitude when graphed against the scan rate, obtained from cyclic voltammetry (CV) at different potential scan rates, in phosphate buffered saline (PBS) solution (0.2 M, pH 7.4) with Ag/AgCl reference electrode. CV was performed using an eDAQ e-corder (401) and potentiostat/galvanostat (EA 160) with Chart version 5.1.2/EChem version 2.0.2 software (ADInstruments), and a PC. Mechanical testing was carried out using a dynamic mechanical analyzer Q800 (TA Instruments). Thermogravimetric analysis (TGA) was carried out using a thermogravimetric analyzer TGA Q500 (TA Instruments) at a heating rate of 10°C min^{-1} and an air flow rate of 60 cm^3 min^{-1}.

Procedure.— HA–SWNT dispersions were prepared from an aqueous solution of HA (0.4 wt %) containing SWNT in a ratio of 2:3, which was ultrasonicated using pulse (2 s on, 1 s off) for 30 min using a high power sonic tip (500 W, 30% amplitude). HA–SWNT–PEI composite fibers were prepared from an HA–SWNT dispersion, 2:3 (0.2 wt %), utilizing a rotating PEI coagulant solution (5 wt % in methanol). Following coagulation, fibers were washed with methanol before drying in ambient conditions. CHIT–SWNT–PEI fibers were produced from a CHIT–SWNT dispersion, 2:1 (0.3 wt %), and PEI coagulant solution in a similar manner to the HA–SWNT–PEI fibers. HA–SWNT and CHIT–SWNT fibers were produced by injecting the respective dispersions into a rotating coagulant solution of acetone. Following coagulation, fibers were dried in ambient conditions.

Results

The most common means of obtaining relatively concentrated CNT dispersions consists of using low molecular weight surfactants as dispersants in water. Biomolecules such as CHIT and HA (Fig. 1)

* Electrochemical Society Active Member.
[z] E-mail: Carol.Lynam@dcu.ie

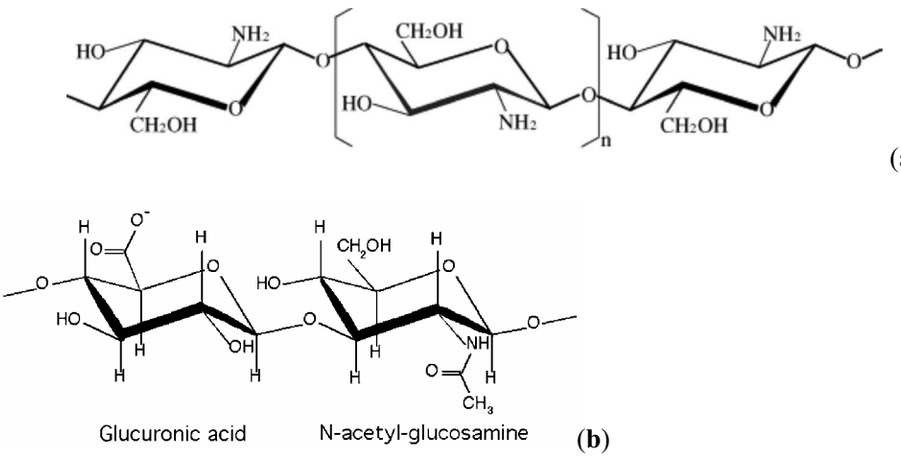

Figure 1. Structures of biomolecules used as SWNT dispersant: (a) CHIT and (b) HA.

are excellent dispersants for CNTs, usually at lower concentrations than surfactants.[13] We prepared SWNT–biomolecule dispersions by sonicating a given amount of SWNT in an aqueous solution of biomolecule (CHIT or HA) to form highly stable biomolecule–SWNT suspensions. In the case of CHIT as a dispersant, a homogeneous dispersion was obtained with a concentration of 0.3% by weight of SWNTs and employing a 2:1 ratio by weight of CHIT–SWNT. Dispersions differing from this concentration and ratio contained large clusters, between 50 and 100 μm, of nondispersed SWNTs. This is in contrast to dispersions made with HA.[13] In the case of HA as a dispersant, concentrations of up to 0.6% by weight of SWNTs were possible. To obtain a homogeneous dispersion, at least a 2:3 ratio by weight of biomolecule–SWNT was necessary.

The affinity for SWNTs and permissiveness as a substrate for neuronal growth led us to consider employing PEI as the coagulant in the fiber-spinning process. A coagulation drop test indicated that acetone is also a suitable coagulant for the dispersions. Because acetone has a low-boiling point and high vapor pressure, it is easily removed from the fiber, resulting in a biocompatible structure. Processing these biomolecule–SWNT dispersions by injection into a flowing stream of polymer solution/solvent produces gel fibers containing SWNTs. As a result of the diffusion of the PEI into the fiber during the coagulation process, cylindrical fibers were formed. Ribbonlike fibers formed in the case of acetone as a coagulant.

To achieve optimal spinning conditions, the influence of experimental variables, i.e., concentration of a coagulant (between 5 and 40% w/v for PEI), time spent in the coagulation bath (between 5 and 60 min), and the rate of injection into the coagulation bath (with injection rate between 100–250 mL/h and coagulation bath rotation rate between 20–40 rpm), were investigated. Employing injection rates and spinning speeds found to be most favorable (rotation speed of 25 rpm; injection rate of 250 mL/h for PEI and 100 mL/h for acetone), the SWNT–biomolecule dispersions were spun into a coagulation bath to form CNT biofibers. The coagulation bath consisted of either PEI in methanol (5 wt %) or acetone. Fiber lengths of up to several meters could be made using optimal conditions; however to avoid entanglement in the rotating coagulation bath, typical fiber lengths were 10 cm.

We obtained uniform cylindrical HA–SWNT–PEI and CHIT–SWNT–PEI fibers with typical diameters of 80 μm. In contrast HA–SWNT and CHIT–SWNT fibers coagulated by acetone were ribbonlike and had typical widths of 70 μm and thicknesses of 50 μm. Biomolecules have been shown to affect the assembly of CNTs, e.g., HA and denatured DNA are effective at stabilizing CNTs leading to suspensions that are isotropic.[13,17] Injecting the SWNT dispersion into the flowing stream of polymer solution mimics the conditions in solutions of rigid polymers or anisotropic colloids.[18] As a result, both biomolecule-assisted and flow-induced alignment of the nanotubes are expected in the direction of the fluid velocity, which is parallel to the fiber axis. SEM images reveal that the CHIT–SWNT–PEI fibers have a corrugated surface, with the axis of corrugation approximately aligned parallel to the fiber axis. These corrugations (typically 0.3–1 μm) are also observed on the HA–SWNT–PEI, HA–SWNT, and CHIT–SWNT fibers, with SEM images suggesting a rougher surface structure than for the CHIT–SWNT–PEI fiber. Images of fractured ends of the fibers indicate the presence of SWNT bundles coated with a biomolecule dispersant or PEI and that a large majority of the SWNTs are aligned along the fiber axis.

Raman spectroscopy (Fig. 2) has confirmed the presence of CNTs in the fibers. High resolution Raman spectroscopy measurements of the radial breathing modes (RBMs) of SWNTs was carried out on the raw SWNT powder used to make the dispersions, SWNT–biomolecule dispersions, and the fibers produced. The spectra (representative spectra are shown in Fig. 2) indicate that a significant interaction takes place between the nanotubes and each biomolecule used as a dispersant. An upshift in the RBM peaks between 3 and 5 cm^{-1} has been observed for the SWNT–biomolecule dispersions and between 5 and 7 cm^{-1} for the SWNT–biofibers. The positions of the D and G bands for raw nanotubes, dispersions, and fibers are within the 4 cm^{-1} variation, which is not significant enough to imply doping of the nanotubes by the biomolecules.[19] These observations are consistent with debundling as previously reported.[19]

Table I compares the mechanical properties, conductivity, and capacitance values for fibers coagulated under different conditions.

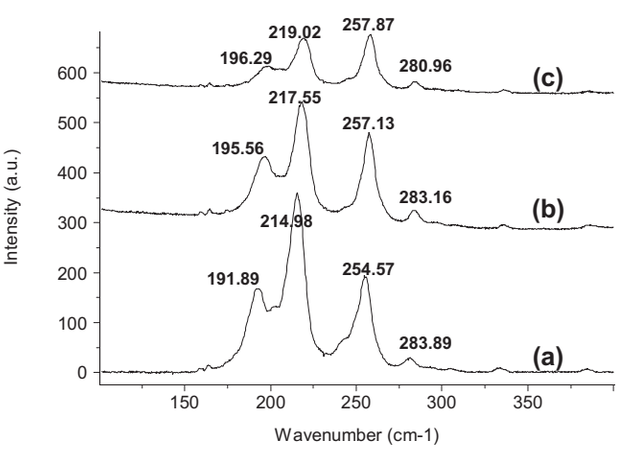

Figure 2. Raman spectra of (a) raw SWNT, (b) HA–SWNT dispersion, and (c) HA–SWNT–PEI fiber confirming the presence of SWNTs.

Table I. Mechanical and electrical properties of SWNT fibers.

	Dispersant				
	HA		CHIT		DNA[a]
Coagulant	PEI	Acetone	PEI	Acetone	PVA
CNT–dispersant ratio	2:3	2:3	1:2	1:2	1:1
Tensile strength (MPa)	120 ± 32	51 ± 10	40 ± 18	60 ± 15	109
Young's modulus (GPa)	8 ± 1	5 ± 1	4 ± 1	8 ± 1	14
Strain (%)	13 ± 1	4 ± 1	3 ± 1	9 ± 1	—
Conductivity (S/cm)	8 ± 1	186 ± 23	0.2 ± 0.1	23 ± 5	0.04
Capacitance (F/g)	4	34	0.006	9	—

[a] Data taken from Ref. 15.

Mechanical testing determined that the average tensile strength of the HA–SWNT–PEI fiber was 120 MPa, while for the CHIT–SWNT–PEI fiber, it was measured as 40 MPa (Table I). The positively charged amino groups of CHIT may repel any cross-linking interaction with the amino groups of PEI in the fiber resulting in a lower tensile strength. A more favorable cross-linking interaction of the PEI amino groups with the negative acidic residues of the glycosaminoglycan chains of HA is possible, which is supported by higher tensile strength values. The average tensile strength of the HA–SWNT fiber was 51 MPa, while for the CHIT–SWNT fiber, it was measured as 60 MPa. We attribute these lower tensile strength values in the acetone-coagulated fibers to the absence of a supporting/cross-linking polymer matrix in the coagulation medium, e.g., PEI. The average tensile strength of the HA–SWNT–PEI fiber is slightly higher than that of the DNA–SWNT–PVA fibers previously reported.[15] A skin–core fiber microstructure was not observed for the fibers reported here unlike CNT–PVA fibers with CNT-enriched inner core and PVA-enriched outer skin.[14,15] A homogeneous distribution of the biomolecule and CNTs was observed on the fiber cross section (Fig. 3). Although the mechanical properties of these fibers do not compare favorably with the commercial high strength fibers used in structural composites, they possess mechanical properties sufficient for use as biosensor electrodes or for the fabrication of substrates for nerve and muscle repair.

The electrical conductivity of previously formed DNA–SWNT–PVA fibers was reported as 0.04 S cm^{-1}. Annealed fibers have been reported with conductivities as high as 167 S cm^{-1},[15] however the increase in electrical properties is accompanied with severe losses in mechanical properties. Conductivities of 0.2 and 8.4 S cm^{-1} were measured for the CHIT–SWNT–PEI and HA–SWNT–PEI fibers produced here, respectively (Table I), which are five times higher and over 2 orders of magnitude higher, respectively, than for the DNA–SWNT–PVA fibers previously reported. It was found that the length of time spent in the coagulation bath did not significantly affect the conductivity of the fibers; however in the case of PEI, a longer rinsing time proved beneficial (e.g., soaking for 3 min resulted in a fiber conductivity of 0.04 S cm^{-1} compared to conductivities of >1.0 S cm^{-1} for 30 min rinses). This is presumably due to a lower insulating PEI content within the fiber, resulting in more electrical connections between CNTs. It was difficult to accurately measure the CNT content of the fibers. An overlap in the decomposition temperature of each component (CNTs and biomolecules) of the composite fiber was observed during TGA (results not shown).

Conductivities of 23 and 186 S cm^{-1} were measured for CHIT–SWNT and HA–SWNT fibers, respectively, the fibers produced from acetone. This is nearly 4 orders of magnitude higher in the case of the HA–SWNT fiber than for the DNA–SWNT–PVA fibers previously reported, while still retaining biofunctionality. We attribute the high conductivities in the acetone-coagulated fibers to the absence of a supporting polymer matrix in the coagulation medium, e.g., PEI. It appears that the amount of biomolecule material remaining in the fiber was sufficient to provide mechanical support, but low

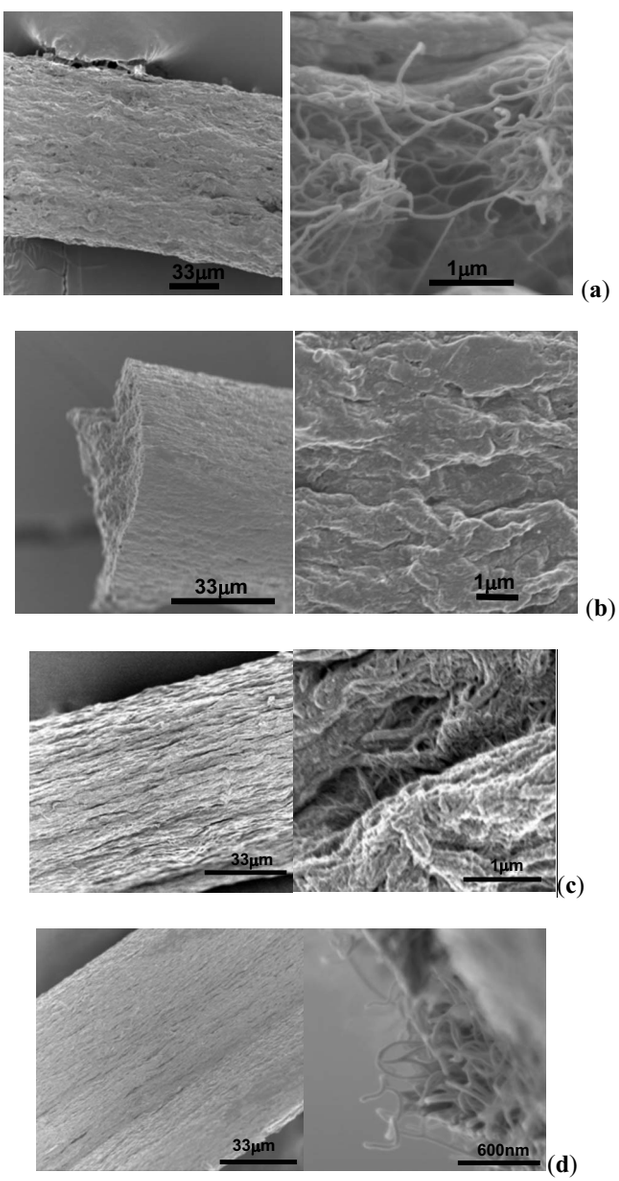

Figure 3. High resolution SEM images of SWNT fibers and of fractured fiber ends, showing differences in fiber morphology: (a) HA–SWNT–PEI, (b) CHIT–SWNT–PEI, (c) HA–SWNT, and (d) CHIT–SWNT fibers.

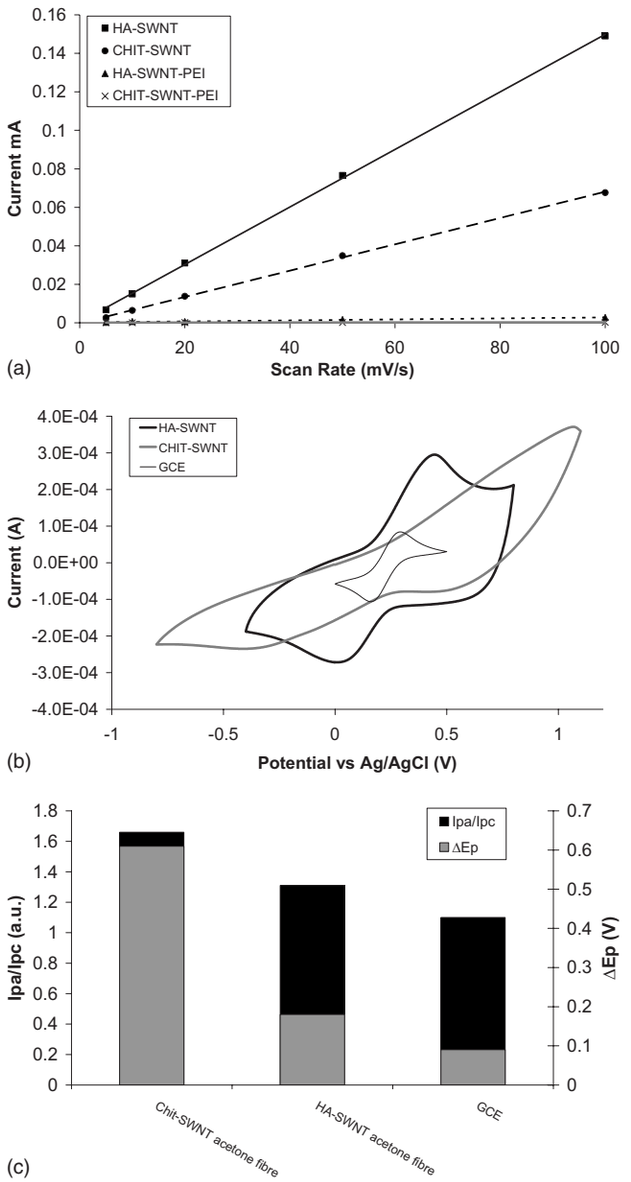

Figure 4. Electrochemical behavior of CNT fibers: HA–SWNT (solid line), CHIT–SWNT (dashed line), HA–SWNT–PEI (dotted line), and CHIT–SWNT–PEI (solid gray line). (a) Plot of current vs scan rate of fibers. (b) Cyclic voltammograms in 1 mM potassium ferricyanide at 100 mV s^{-1}. (c) Effect of fiber composition on the ratios of the anodic peak current to the cathodic peak current (Ipa/Ipc) and the peak potential separation, ΔEp.

enough to allow electrical conductivity via intimate contact between CNT junctions. In support of this, CHIT–SWNT fibers had conductivities up to 8 times lower than that of HA–SWNT fibers, presumably because of the higher biomolecule concentration required to achieve a homogeneous spinning dispersion (0.6 wt % CHIT for 0.3 wt % CNTs). Assuming no CNT and biomolecule loss during fiber formation, the CNT composition of the acetone-coagulated fibers could be estimated based on the concentration of the CNT dispersions. This translates to 60 and 33 wt % CNT content for the HA–SWNT and CHIT–SWNT fibers, respectively.

CV (performed in the physiological medium 0.2 M PBS, pH 7.4), gave responses that indicate that capacitive behavior predominates, irrespective of the coagulation system used. A linear dependence of the current flows on scan rate was observed, and specific capacitance values of 34, 9, and 4 F/g for HA–SWNT, CHIT–SWNT, and HA–SWNT–PEI fibers, respectively, were obtained. However, more resistive CV measurements were observed for CHIT–SWNT–PEI fibers because of their reduced electrical conductivity (giving a specific capacitance of 6 mF/g).

A series of preliminary measurements using 1 mM potassium ferricyanide was carried out to characterize the electrochemical response of these CNT-fiber electrodes. Measurement of the ferricyanide faradaic current as a function of the scan rate was performed on two of the fibers with the highest electrical conductivity (HA–SWNT and CHIT–SWNT) to establish whether the electrochemical reaction was diffusion controlled. Figure 4b shows voltammograms of the fibers HA–SWNT and CHIT–SWNT and a glassy carbon electrode recorded at a scan rate of 100 mV/s. An analysis of the faradaic current obtained resulted in linear plots of I_p vs $v^{1/2}$ over the range studied (5–200 mV/s), indicating that the current is controlled by a semi-infinite linear diffusion in the case of this redox couple. Similarly, a diffusion-controlled electron transfer at these CNT–biofiber microelectrodes was also found for ferrocene monocarboxylic acid and ruthenium hexamine chloride (data not shown). The potential differences (ΔEp) and the ratios of the anodic peak current to the cathodic peak current (Ipa/Ipc of ferricyanide) are compared in Fig. 4c. As expected, as the conductivity of the fibers increases, the peak potential difference as well as Ipa/Ipc decrease and the Ipa/Ipc is closer to 1 with an improvement in reversibility of the couple. Overall, the results presented here demonstrate that acetone-coagulated CNT–biofiber microelectrodes possess sufficient electrical conductivity and a wide working potential range, making them useful for many analytical applications.

While CHIT as a dispersant and PEI as a coagulant produced fibers with higher electrical conductivity than the DNA–SWNT–PVA fibers, it did so at the cost of mechanical properties. HA as a dispersant and PEI as a coagulant provided fibers with the same mechanical properties as the DNA–SWNT–PVA fibers, but with a 2 order of magnitude increase in electrical conductivity. Further increases in conductivity were obtained when acetone was used as the coagulant, but unfortunately to the detriment of mechanical properties.

In summary we have successfully prepared CNT fiber microelectrodes from all biocompatible polymers. While incorporating biofunctionality, the HA–SWNT–PEI fibers compromise little in terms of mechanical properties with a 2 order of magnitude increase in electronic conductivity compared to DNA–SWNT–PVA fibers. With adequate mechanical properties for the intended applications, the HA–SWNT acetone-coagulated fibers have electrical conductivities 4 orders of magnitude higher than the DNA–SWNT–PVA fibers. These fibers may prove useful as biosensor microelectrodes and substrates which support and allow the electrical stimulation of mammalian cells, studies currently under way in our laboratories.

Acknowledgments

The authors gratefully acknowledge the financial support of the Australian Research Council.

University of Wollongong assisted in meeting the publication costs of this article.

References

1. V. Lovat, D. Pantarotto, L. Lagostena, B. Cacciari, M. Grandolfo, M. Righi, G. Spalluto, M. Prato, and L. Ballerini, *Nano Lett.*, **5**, 1107 (2005).
2. H. Hu, Y. Ni, V. Montana, R. C. Haddon, and V. Parpura, *Nano Lett.*, **4**, 507 (2004).
3. M. P. Mattson, R. C. Haddon, and A. M. Rao, *J. Mol. Neurosci.*, **14**, 175 (2000).
4. N. Dubey, P. C. Letourneau, and R. T. Tranquillo, *Biomaterials*, **22**, 1065 (2001).
5. S. A. Makohliso, R. F. Valentini, and P. Aebischer, *J. Biomed. Mater. Res.*, **27**, 1075 (1993).
6. M. E. Manwaring, R. Biran, and P. A. Tresco, *Biomaterials*, **22**, 3155 (2001).
7. A. Lahiji, A. Sohrabi, D. S. Hungerford, and C. G. Frondoza, *J. Biomed. Mater. Res.*, **51**, 586 (2000).
8. L. A. Solchaga, J. E. Dennis, V. M. Goldberg, and A. I. Caplan, *J. Orthop. Res.*, **17**, 205 (2005).
9. G. Haipeng, Z. Yinghui, L. Jianchun, G. Yandao, Z. Nanming, and Z. Xiufang, *J. Biomed. Mater. Res.*, **52**, 285 (2000).
10. B. R. Seckel, D. Jones, K. J. Hekimian, K.-K. Wang, D. P. Chakalis, and P. D.

Costas, *J. Neurosci. Res.*, **40**, 318 (2004).
11. S. Yamane, N. Iwasaki, T. Majima, T. Funakoshi, T. Masuko, K. Harada, A. Minami, K. Monde, and K. Nishimura, *Biomaterials*, **26**, 611 (2005).
12. F. L. Mi, S. S. Shyu, C. K. Peng, Y. B. Wu, H. W. Sung, P. S. Wang, and C. C. Huang, *J. Biomed. Mater. Res. Part A*, **76**, 1 (2006).
13. S. E. Moulton, M. Maugey, P. Poulin, and G. G. Wallace, *J. Am. Chem. Soc.*, **129**, 9452 (2007).
14. B. Vigolo, A. Penicaud, C. Coulon, C. Sauder, R. Pailler, C. Journet, P. Bernier, and P. Poulin, *Science*, **290**, 1331 (2000).
15. J. N. Barisci, M. Tahhan, G. G. Wallace, S. Badaire, T. Vaugien, M. Maugey, and P. Poulin, *Adv. Funct. Mater.*, **14**, 133 (2004).
16. E. Muñoz, D.-S. Suh, S. Collins, M. Selvidge, A. B. Dalton, B. G. Kim, J. M. Razal, G. Ussery, A. G. Rinzler, M. T. Martínez, et al., *Adv. Mater. (Weinheim, Ger.)*, **17**, 1064 (2005).
17. S. Badaire, C. Zakri, M. Maugey, A. Derre, J. N. Barisci, G. Wallace, and P. Poulin, *Adv. Mater. (Weinheim, Ger.)*, **17**, 1673 (2005).
18. M. Doi and S. F. Edwards, *The Theory of Polymer Dynamics*, Oxford University Press, New York (1986).
19. M. S. Dresselhaus, A. M. Rao, and G. Dresselhaus, in *Encyclopaedia of Nanoscience and Nanotechnology*, Vol. 9, H. S. Nalwa, Editor, p. 307, American Scientific Publishers, CA (2004).